Effect of Interface Structure on the Microstructural Evolution of Ceramics

Wook Jo, Doh-Yeon Kim,* and Nong-Moon Hwang
School of Materials Science & Engineering and Center for Microstructure Science of Materials, Seoul National University, Seoul 151-744, Korea

The interface atomic structure was proposed to have a critical effect on the microstructure evolution during sintering of ceramic materials. In liquid-phase sintering, spherical grains show the normal grain growth behavior without exception, while angular grains often grow abnormally. The coarsening process of spherical grains with a disordered or rough interface atomic structure is diffusion-controlled, because there is little energy barrier for atomic attachments. On the other hand, kink-generating sources such as screw dislocations or two-dimensional (2-D) nuclei are required for angular grains having an ordered or singular interface structure. Coarsening of angular grains based on 2-D nucleation mechanism could explain the abnormal grain growth behavior. It was also proposed that densification process is closely related to the interface atomic structure. Enhanced densification by carefully chosen additives during solid state sintering was explained in terms of the grain boundary structural transition from an ordered to a disordered open structure.

Keywords: Interface Structure, Sintering, Microstructure, Grain Growth, Densification

I. INTRODUCTION

Microstructure control is a key issue in materials engineering because almost all the material properties are dependent upon their internal microstructures. Therefore, the microstructural evolution during the sintering of ceramic materials has been studied extensively. In alumina, for instance, it is well known[1] that when pure powder compacts are sintered, some grains grow extensively to an enormous size with pores trapped within those large grains. Usually, a limited number of grains grow much faster than the average, and this phenomenon is often referred to as abnormal grain growth (AGG). A fully dense and fine-grained Al_2O_3 microstructure can be achieved when a very small amount of MgO is added, and this subject was reviewed by Bennison and Harmer.[2]

The sintering process involves both densification and grain growth, which occur basically through atomic movements in the bulk or at the interfaces.[3–6] The densification process is the replacement of solid/vapor interfaces either by solid/solid interfaces (solid state sintering) or by solid/liquid interfaces (liquid-phase sintering). On the other hand, grain growth is related to the minimization of total interfacial area by interface migration. In this respect, it is well-known that the sintering is an interface related process in terms of the driving force and kinetics, dating back at least to Herring's celebrated papers[7,8] on sintering.

In the mean time, a comprehensive analysis of interfaces at an atomistic level was performed by Burton, Cabrera and Frank (BCF)[9] in 1951. They adopted the terrace-ledge-kink (TLK) model to describe the atomic structures of surfaces. According to their description, low index surfaces are atomically smooth at moderate temperatures and referred to as singular, because singularities or cusps are present at these orientations in the γ-plot (a polar diagram where the length of the radius vector is proportional to the value of surface energy, γ). A vicinal surface, which is slightly different in orientation from a singular surface, consists mainly of flat regions called terraces and widely spaced atomic ledges with kinks. BCF[9] proposed that there should be a transition of surfaces from an atomically smooth to a rough state at a certain temperature. Jackson[10] further developed the theory of a roughening transition in the case of solid-liquid interfaces. He identified key parameters that determine whether an interface is atomically smooth or rough for a given material.

Indeed, Herring[7] pointed out in his classic paper that the interface atomic structure would have a critical influence on the sintering phenomena. To establish the scaling law of sintering process, he assumed that the interface of materials is atomically rough with isotropic surface energy, and suggested that his analysis would be incorrect if an atomically smooth interface is considered. However, it is fairly recently that systematic analyses on the role of the interface structure during sintering have been performed. The interface structure is of interest these days not only because of its implication for microstructure control but also because of its relationship with the material properties.

Consideration of the interface structure can solve some puzzling microstructural evolutions that have not been understood clearly before. For example, AGG of angular solid grains during the liquid-phase sintering can be approached by considering that the solid/liquid interface of angular grains is atomically smooth. On the other hand, the grain boundary, which is known as a source or sink of vacancies, plays an important role in densification process during the solid-state sintering. Vacancy diffusion is expected to depend strongly on the grain boundary structure; its rate would be much higher in a disordered grain boundary than in an ordered one. This concept may be applied to the additive effect during the solid-state sintering. When the grain-boundary structure is changed from singular to rough by some additives, the densification rate will be enhanced.

As a matter of course, the sintering process is too com-

Report Documentation Page

Form Approved
OMB No. 0704-0188

1. REPORT DATE	2. REPORT TYPE	3. DATES COVERED
06 NOV 2007		

4. TITLE AND SUBTITLE	5a. CONTRACT NUMBER
Interface and Healing and Repair of Ceramics	**FA48690610105**
	5b. GRANT NUMBER
	5c. PROGRAM ELEMENT NUMBER
6. AUTHOR(S)	5d. PROJECT NUMBER
Doh-Yeon Kim	5e. TASK NUMBER
	5f. WORK UNIT NUMBER
7. PERFORMING ORGANIZATION NAME(S) AND ADDRESS(ES)	8. PERFORMING ORGANIZATION REPORT NUMBER
Seoul National University,Silim-dong, Kwanak-Gu,Seoul 151-744,KR,151-744	**N/A**
9. SPONSORING/MONITORING AGENCY NAME(S) AND ADDRESS(ES)	10. SPONSOR/MONITOR'S ACRONYM(S)
	11. SPONSOR/MONITOR'S REPORT NUMBER(S)

12. DISTRIBUTION/AVAILABILITY STATEMENT

Approved for public release; distribution unlimited.

13. SUPPLEMENTARY NOTES

14. ABSTRACT

The interface atomic structure was proposed to have a critical e®ect on the microstructure evo- lution during sintering of ceramic materials. In liquid-phase sintering, spherical grains show the normal grain growth behavior without exception, while angular grains often grow abnormally. The coarsening process of spherical grains with a disordered or rough interface atomic structure is di®usion-controlled, because there is little energy barrier for atomic attachments. On the other hand, kink-generating sources such as screw dislocations or two-dimensional (2-D) nuclei are re- quired for angular grains having an ordered or singular interface structure. Coarsening of angular grains based on 2-D nucleation mechanism could explain the abnormal grain growth behavior. It was also proposed that densi¯cation process is closely related to the interface atomic structure. Enhanced densi¯cation by carefully chosen additives during solid state sintering was explained in terms of the grain boundary structural transition from an ordered to a disordered open structure

15. SUBJECT TERMS

16. SECURITY CLASSIFICATION OF:			17. LIMITATION OF ABSTRACT	18. NUMBER OF PAGES	19a. NAME OF RESPONSIBLE PERSON
a. REPORT	b. ABSTRACT	c. THIS PAGE			
unclassified	**unclassified**	**unclassified**		**18**	

plicated to be described in terms of the interface structures alone. The process also depends on the characteristics of individual systems such as atomic bonding, possible subsidiary reactions, phase stability, diffusion kinetics, and so forth.[3–6] However, we try to focus on the interface atomic structure and its effect on the grain growth and densification during the sintering process. In that regard, we will briefly introduce the current understanding on interface atomic structures, followed by reviews and comments on contemporary works related to grain growth and densification.

II. INTERFACE ATOMIC STRUCTURE

The interfaces involved in the sintering process are solid/vapor, solid/liquid and solid/solid, but they have many common features at an atomistic level. For example, the ideas developed for the TLK model in solid/vapor interface (surface) are equally applicable to the other interfaces.[11,12] Identical treatment can be applied, particularly when it comes to the solid/vapor and the solid/liquid interfaces. Therefore, both interfaces hereafter will be treated in a similar manner and are simply referred to as surfaces. On the other hand, the solid/solid interface, more specifically the grain boundary will be treated separately, because it has a couple of distinctive features from a structural point of view. Before going into details, let us briefly mention how the interface structure can affect grain growth and densification during sintering.

Coarsening, or Ostwald ripening of solid grains dispersed in a liquid matrix is driven by the capillarity effect. That is, grains which are smaller than average go into solution and the larger ones grow. During this solution-reprecipitation process, the growth of each solid grain is affected significantly by the surface structure. Since reversible transfer of atoms occurs only at kinks,[13,14] the kinetics of atomic attachment to a growing interface depends upon the density of kinks on that interface. It follows that the atomically smooth interface, which is characterized by the limited number of kinks, tends to have interface-controlled growth, and kink-generating sources such as screw dislocations or 2-D nuclei are needed for growth. On the other hand, an atomically rough interface, which is characterized by infinite inherent kinks, tends to have diffusion-controlled growth.

A. Surface Structure Fundamentals

It is now well established that the surface structure can be categorized into two different types; atomically smooth and rough. Consider an atomically smooth low-index surface (Fig. 1(a)) with unit normal n and a vicinal surface (Fig. 1(b)) with a slightly different orientation, $n + \delta n$, at a finite temperature. As long as δn is small enough, the vicinal, or stepped surface will show the same structure as shown in Fig. 1(a) except for the presence of widely separated steps, or ledges. In this case, a certain amount of excess energy arises due to the presence of steps, and its value per unit length is referred to as the step free energy, ϵ. Note that the steps cannot be generated by statistical thermal excitation.[9] Therefore, the surface energy of a vicinal surface, $\gamma(n + \delta n)$, regardless of the sign of δn, will be higher than $\gamma(n)$ by an amount asymptotically proportional to the density of the steps.[8]

Since the low index surface has a local minimum γ value, the γ-plot will have a cusp at that orientation n.[8,15–20] This indicates that there should a certain range of missing crystallographic orientations around the cusp in equilibrium crystals.[21–24] Therefore, when a crystal is bounded by atomically smooth planes, its equilibrium shape will be polyhedral with the lowest energy planes. On the other hand, the rough surface schematically illustrated in Fig. 1(c) is characterized by thermally generated innumerable kinks. When a crystal is bounded by rough surfaces, the surface energy is isotropic with no missing orientations. It is obvious in this case that the equilibrium shape becomes a sphere, which can be considered as a polyhedron with an infinite number of planes.

One of the important theoretical achievements made in surface physics is the surface structural transition from a low-temperature atomically smooth state to a high-temperature rough one. The former has an enthalpy-dominant ordered structure, whereas the latter has an entropy-dominant disordered one. In this approach, the surface is considered to undergo a structural transition like a bulk.[23,25–27]. Many studies have been carried out over the last few decades on this subject and several excellent reviews are currently available.[23,25–29]

The transition of a surface structure from singular to atomically rough was not clearly demonstrated experimentally until recent observations by scanning tunneling microscope.[30–34] Note that the surface transition has no observable heat singularity, which is a typical feature of thermodynamic phase transformations.[35] Furthermore, the extent of the transition is limited to only a few atomic layers from the surface level. Because of these unique features of the surface roughening transition, most studies on the subject have been purely theoretical and have focused on predicting the transition temperature T_R, above which a singular surface transforms to a rough one. In definition, T_R is the temperature where ϵ becomes zero.

A simple theoretical approach to evaluate T_R can be described as follows.[36] Consider a monatomic zig-zag shaped step on a (001) surface of a simple cubic crystal as shown in Fig. 2. The average direction of the step was chosen to make 45° angle with the row of atoms. Here, the total length of the step becomes $2L$, which means that there are 2^{2L} configurations available. Thus, the configurational entropy due to the step is given as

$$S = k \ln 2^{2L} = 2Lk \ln 2, \tag{1}$$

where k is the Boltzmann constant. On the other hand,

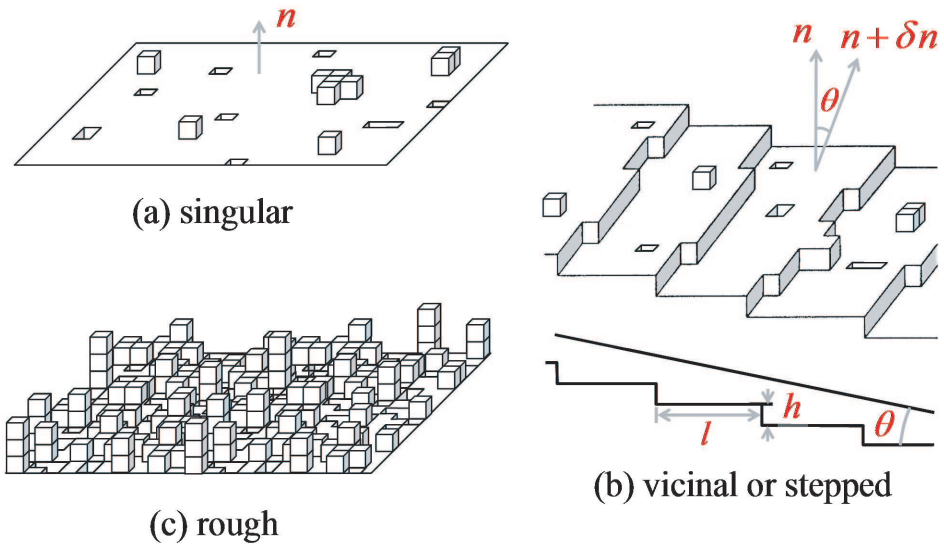

FIG. 1: Schematic illustrations of (a) singular, (b) vicinal or stepped, and (c) rough surface.

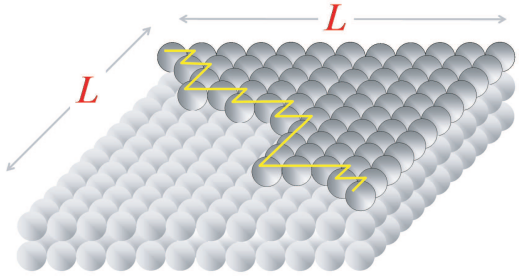

FIG. 2: Schematic illustration showing a step on a surface with a simple cubic symmetry.

when the formation enthalpy of the step per bond, ψ, is assumed constant, the total step free energy is given by

$$E = 2L\psi - 2LkT\ln 2. \tag{2}$$

The step free energy per unit length can then be obtained as follows.

$$\epsilon = \psi - kT\ln 2. \tag{3}$$

This equation implies that ϵ becomes zero at a certain temperature, which is defined as the roughening transition temperature, T_R, and is expressed as

$$T_R = \frac{\psi}{k\ln 2}. \tag{4}$$

In the mean time, ϵ can be evaluated with respect to γ using the TLK model of a surface from Fig. 1(b). The energy of a stepped surface inclined at an angle θ to the low index surface can be written as[37]

$$\gamma(\theta) = \gamma_0\cos\theta + \frac{\epsilon}{h}\sin\theta. \tag{5}$$

where γ_0 is the interface free energy of the terrace plane, h is the step height and l is the mean separation distance of the ledges. The main result of Eq. 5 is that a plot of γ versus θ has a cusp when θ equals zero and the slope near this cusp is proportional to ϵ, *i.e.*

$$\left[\frac{d\gamma(\theta)}{d\theta}\right]_{\theta\to 0} = \frac{\epsilon}{h}. \tag{6}$$

Therefore, ϵ can be estimated by measuring the slope of the γ-θ plot near the low index planes.

Since γ for an isotropic spherical crystal does not vary with respect to θ, it is evident that ϵ is zero. On the other hand, for angular grains ϵ should have a finite value, because there should be cusps at angles corresponding to the crystallographic planes with the local minimum values in γ-θ plot. In this case, the Wulff theorem[15–19] predicts that if planes are drawn perpendicular to the radius vectors where they cut the γ-plot, the innermost envelope of these planes corresponds to the equilibrium crystal shape. As a result, the deeper the cusps become, the fewer planes will appear in the equilibrium crystal. This means in turn that ϵ is inversely proportional to the number of planes that bound the equilibrium crystal. Furthermore, we can predict that crystals with angular corners or sharp edges due to deeper cusps in the γ-θ plot have a higher ϵ than the corner- or edge-rounded crystals. Figure 3 shows a change in the equilibrium crystal shape from cubic to spherical with increasing temperature (*i.e.* with decreasing ϵ.)[23]

Although the roughening transition is much more complicated than that described above, the linear dependence of ϵ on temperature predicted by Eq. 3 is in good agreement with experimental observations except when the temperature is very close to T_R.[38] On the other hand, T_R is known to depend on the surface orientation.[36] It

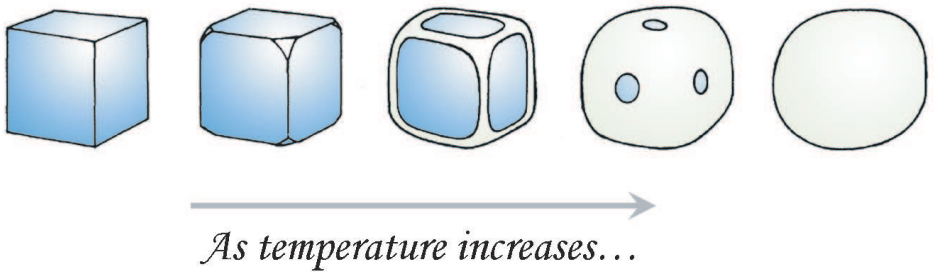

FIG. 3: Change in an equilibrium crystal shape with temperature from a cube to a sphere. Note that the change in the crystal shape is related to the decrease in step free energy.[23]

is generally accepted that the higher the crystallographic index of the plane, the lower the T_R. This suggests that the rounded edges or corners of the crystal shown in Fig. 3 could be in an atomically roughened state. However, a recent investigation[39] on this subject claims that all the surfaces appearing in the equilibrium crystal have an identical T_R, *i.e.* T_R is independent of the crystallographic orientation. Therefore, the rounded edges or corners of the crystal shown in Fig. 3 are not in an atomically rough state. Instead, the rounded parts are composed of micro-facets or steps, as was observed experimentally.[40]

So far, except for the possible presence of ledges when the surface is vicinal, the structure of a crystal surface has been considered to be free from any reconstructions or relaxations.[12] However, the reconstruction process plays an important role in determining the equilibrium crystal shape, and details can be obtained from recent works in the field of surface science.[41–45] In addition, various surface defects such as dislocations or twins should be present in real crystals. As will be shown in subsequent sections, these defects have a critical influence on the microstructure developments during sintering. Besides, the adsorption effect by the impurity atoms on the surface was ignored for simplicity. This topic can also be referred to the previous publications.[41–45]

B. Grain Boundaries

The grain boundaries in polycrystalline materials have a certain degree of complexity, because they are formed by two surfaces of different orientation. Therefore, their macroscopic characterization requires more complicated mathematical descriptions than in dealing with free surfaces. For example, eight degrees-of-freedom (DOFs), namely five macroscopic DOFs related to misorientation and inclination and three microscopic or translational DOFs related to the boundary structure are necessary to describe the grain boundary completely.[46] Note that just a single DOF of a surface normal is needed to define the surface (*i.e.* solid/vapor and solid/liquid interfaces).

As was discussed in the previous section, the surface energies of a crystal are easy to determine as long as its equilibrium shape is known. However, there are no definite and systematic rules for predicting the lowest energy configuration for a specific grain boundary because they cannot be treated as a thermodynamic equilibrium entity. Nevertheless, there are a couple of general consensus, and they are well-documented in references[46,47] and the citations therein.

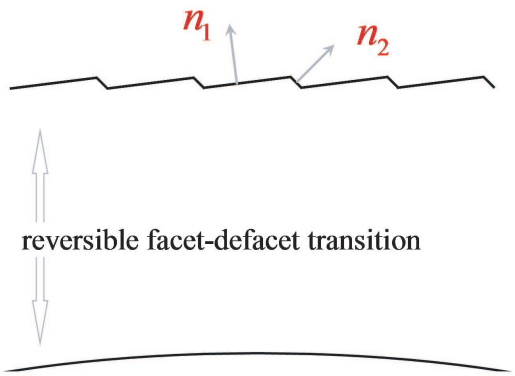

FIG. 4: Schematic illustration showing the reversible facet-defacet transition of grain boundary.

First, low-angle grain boundaries can be represented by a periodic array of edge dislocations.[48] Second, the grain boundary energies have cusped minima at certain misorientations, even when its composing free surfaces show no cusp at the corresponding orientation.[49–51] Several models such as coincidence site lattice (CSL) have been proposed to explain those cusped minima in the grain boundary energy. The grain boundary energy is always smaller than the related free surface energy because it contains fewer broken bonds than surfaces.[52,53]

Apart from their structural complexity, the grain boundaries are also known to undergo a structural transition from singular to rough.[54–57] as shown schematically in Fig. 4. The enthalpy-dominant facet structure is ordered and compact whereas the entropy-dominant defacet structure is disordered and open. The vacancy diffusion along the latter is expected to be much faster than that along the former. Therefore, the pore removal

rate through the grain boundaries would be much higher in the defacet structure than in the facet structure. In some systems during solid-state sintering, the densification behavior changes abruptly by an incorporation of a small amount of dopants. These phenomena may be approached by a grain boundary structural transition.

III. GRAIN GROWTH DURING SINTERING

For the sake of simplicity, let us first discuss the relationship between the interface structure and grain growth during liquid-phase sintering *i.e.* the sintering of a powder compact containing a small amount of a deliberately added liquid-phase. For the grain growth study, the specimen prepared by liquid-phase sintering has a decisive advantage because only the solid-liquid interface is involved particularly when the dihedral angle is zero. Another advantage is that the shape of growing grains is usually near thermodynamic equilibrium so that the interface atomic structure can be rather easily predicted.[58,59] Note also that most ceramic products such as abrasives, capacitors and magnets are fabricated with a liquid-phase being present during sintering.[60] Furthermore, investigations using high resolution electron microscopy showed that even solid-state sintered ceramic products usually have a thin intergranular liquid film during sintering.[61,62] In most ceramics, therefore, it can be considered that grain growth occurs by the migration of solid-liquid interface.

In the typical microstructure of liquid-phase sintered materials, solid grains with a range of size distribution are dispersed in a liquid matrix. Therefore, the smaller particles with higher solubility in the liquid matrix shrink and the larger ones grow. The theoretical aspect of this process, usually referred to as Ostwald ripening, was rigorously treated in the classic paper by Lifshitz and Slyozov[63] and Wagner[64]; the treatment is called the LSW theory. When the coarsening process is controlled by diffusion through the liquid medium, the grain size distribution normalized by the average size is self-regulating *i.e.* it remains constant as the average size increases, and the growth kinetics of the average grain size has a $t^{1/3}$ time dependence. Indeed, the grain growth process during liquid-phase sintering such as W-Ni,[65] MgO-V_2O_5,[66] VC-Co,[67] and Mo-Ni[68] was observed to follow the $t^{1/3}$ law, as predicted for the diffusion-controlled growth mechanism. The growth patterns of Mo grains revealed by severe etching[68] are an experimental evidence for the theoretically predicted Ostwald ripening. In these materials, the normalized grain size distribution remains constant even after an extensive annealing, *i.e.* no AGG was observed to occur. The overall coarsening behavior is in good agreement with the LSW or modified LSW theory.[69] The shapes of the W, MgO, VC and Mo grains dispersed in a liquid matrix are all more or less spherical, which indicates that their interface structures are atomically rough.

On the other hand, AGG during liquid-phase sintering has been extensively studied in the WC-Co system, which is widely used for cutting tools.[70,71] The presence of a few WC grains with a substantially larger size than the average has a very harmful effect on the strength of this material. A small amount of TaC, VC or other carbides is usually added to inhibit AGG in WC-Co.[72] Note that the shape of the WC grains is angular. Indeed, it is interesting that AGG has never been observed in a system composed of spherical grains with isotropic surface energy. In contrast, AGG has been frequently observed to occur in systems composed of angular grains with anisotropic surface energy. Typical examples are Y-Ba-Cu-O superconductor,[73] ferrite,[74,75] $BaTiO_3$,[76,77] Si_3N_4,[78,79] SiC,[80,81] Al_2O_3,[82,83] B_4C[84] and mullite[85]. The boundaries of the abnormally large grown grains are apparently perfectly straight without exception. In the NbC-Co system,[86] the grain growth behavior changes from AGG to NGG with the addition of boron which causes the grain shape to change from angular to spherical. This strong correlation between AGG and the grain shape provides an important insight that the mechanism for AGG is closely related to the interface atomic structure.

A. Effect of 2-D Nucleation on Coarsening Behavior of Angular Grains during Liquid-Phase Sintering

In single crystal growth, the correlation between the crystal shape and its growth behavior has been extensively studied and now well-established.[12,14,87–89] In analogy, the relationship between grain shape and its growth behavior should also hold during sintering process.[6,8,90–101] Spherical grains with isotropic surface energy have an atomically rough interface while angular grains with anisotropic surface energy have an atomically smooth interface. For spherical grains, therefore, the attachment or detachment of atoms at the interface is relatively easy so that the grain growth process in a liquid matrix is controlled by diffusion. On the other hand, when the grains are angular and faceted, the attachment of an atom to the interface produces excess broken bonds, which increases the chemical potential. Therefore, a significant energy barrier for the atomic attachment to the surface is expected, which results in an interface reaction controlled coarsening process.

Figure 5 shows the variation in the growth rate of a grain or a crystal as a function of driving force. For the grains dispersed in a liquid matrix, the driving force for the growth of a grain of size r is given by[5,12,88,106,107]

$$\Delta G_v = 2\gamma_{sl} V_m \left(\frac{1}{r*} - \frac{1}{r} \right), \tag{7}$$

where γ_{sl} and V_m are the solid-liquid interfacial energy and the molar volume, respectively. r^* is a size of grains that are neither dissolving nor growing. For spherical grains having atomically rough interfaces, the growth

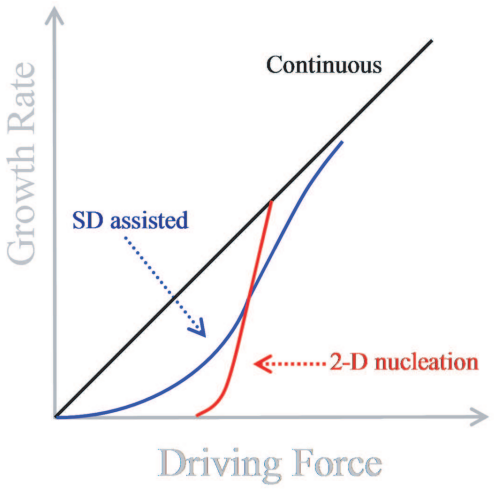

FIG. 5: Interface migration velocity as a function of the driving force; the black line represents the diffusion controlled case (continuous growth). Note that the growth rate remains negligible up to a critical driving force in the case of 2-D nucleation process. When there are defects such as screw dislocations (SD), the growth rate is higher than that of the 2-D nucleation when the driving force is relatively small.[102–105]

process is controlled by diffusion and, therefore, all the grains larger than r^* can grow, as is shown in Fig. 5 (continuous growth). On the other hand, in the case of angular grains the growth process is controlled by 2-D nucleation, which means that the growth rate will remain almost zero and increase abruptly when ΔG_v exceeds a certain critical value.[92,108–110] This may explain AGG, because only those large grains having enough driving force can grow by the 2-D nucleation process. Recently, this possibility has been studied not only experimentally in various ceramic systems[77–79,82,86,92,111–116] but also by a numerical analysis.[108] In fact, Wynblatt *et al.*[90,117] already pointed out that the "nucleation inhibited" growth of faceted particles can satisfactorily account for the coarsening of platinum particles on an alumina substrate. Although they did not explicitly mention the AGG behavior, their works are believed to lay the basis for the 2-D nucleation controlled coarsening process.

As was previously noted, growth steps which provide kink sites cannot be generated by thermal fluctuations, but are the result of nucleation. Assuming that a 2-D nucleus on an atomically flat surface is a circular disk with atomic height h and radius R, the free energy change associated with the nucleation is given as[12,88,106]

$$\Delta G = 2\pi R\epsilon - \pi h R^2 \Delta G_v. \tag{8}$$

Therefore, the energy barrier for 2-D nucleation, which is given by the maximum value of Eq. 8, can be written as

$$\Delta G^*_{2D} = \frac{\pi \epsilon^2}{h\Delta G_v}. \tag{9}$$

Since the nucleation rate is proportional to $\exp(-\Delta G^*_{2D}/kT)$, a small variation in activation energy will bring about a notable change in the coarsening process. In this regard, AGG may occur when ϵ is relatively high because only a few large grains with sufficient driving force can grow. When ϵ is low, many grains can grow simultaneously so that a uniform grained microstructure will be obtained. In contrast, when ϵ is quite high, a fine-grained microstructure is obtained because the overall coarsening process is limited. Note that the variation of ϵ is related to the crystal shape (Fig. 3).

These aspects are clearly revealed from a computer-aided numerical analysis shown in Fig. 6. In this analysis, the kinetic roughening is assumed. This means that when the driving force is fairly large, the growth rate by 2-D nucleation becomes identical to that of the continuous growth. The other conditions for analysis are the same as those reported by Kang *et al.*[108] When the step free energy is 10% of the solid/liquid interface energy ($\epsilon = 0.1h\gamma$) as shown in Fig. 6(a), many grains can grow simultaneously, and a rather uniform-grained microstructure will develop. Figure 6(b) shows the typical microstructure of AGG when the step free energy is equal to 20% of the solid/liquid interface energy ($\epsilon = 0.2h\gamma$). Finally, when the step free energy corresponds to 30% of the solid/liquid interface energy ($\epsilon = 0.3h\gamma$) as in Fig. 6(c), the growth of most grains is significantly inhibited, resulting in a fine-grained microstructure. This result shows that the coarsening by 2-D nucleation mechanism can lead to AGG when the value of ϵ ranges from about 10 to 30% of the solid/liquid interface energy. It also shows that the grain growth can be inhibited by increasing ϵ, which can be accomplished either by decreasing temperature or by adding some impurity atoms. The related experimental results will be treated later.

It can be argued that the screw dislocation-assisted growth might also be the cause of AGG.[110] Indeed, when only a limited number of grains contain screw dislocations, these grains will grow exclusively over other grains. Chung *et al.*,[119,120] carried out a model experiment using a $SrTiO_3$ single crystal with its top surface containing more dislocations than the bottom surface. They showed that the growth rate of the single crystal towards a $SrTiO_3$ powder compact is noticeably enhanced by the dislocations particularly when an intergranular Ti-rich liquid is present.

As shown in Fig. 3, ϵ can be estimated qualitatively from the shape of the grains. Choi *et al.*[114] showed that the shape of solid grains in liquid phase sintered $(Nb_{1-x}Ti_x)C$-Co alloys changes from rounded to sharp corners with increasing Ti concentration, as shown in Fig. 7(a)-(c). The SEM microstructures of the three-dimensional shape of solid grains shown in Fig. 7(a)-(c) were prepared by selective etching of the Co-rich liquid matrix after sintering at 1500 °C for 64h. Figure 7(a)-(c) show that the ϵ of solid grains increases with increasing Ti concentration.

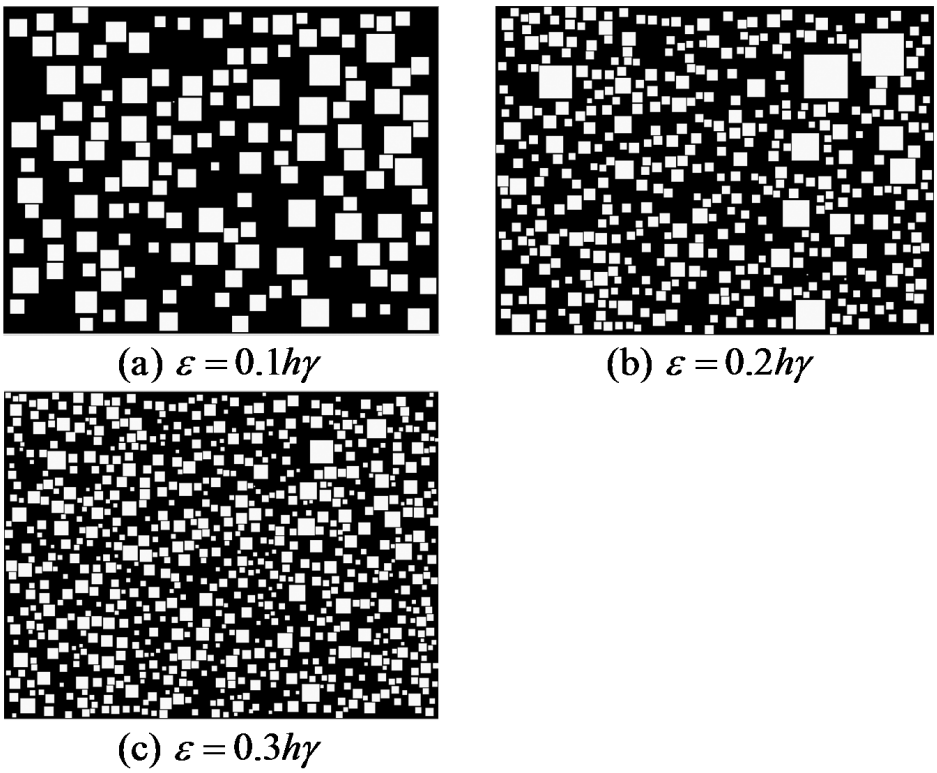

FIG. 6: Results of computer-aided numerical analysis on the microstructure evolution during liquid-phase sintering as a function of the step free energy, ϵ.

Corner and edge rounded grains with low ϵ (Fig. 7(a)) showed a uniform grained structure, as shown in Fig. 7(d). On the other hand, grains with sharp corners (Fig 7(b) and (c)) exhibited AGG (Fig. 7(e) and (f), respectively). In Fig. 7(e), where ϵ is expected to be higher than that of Fig. 7(d), only a few grains grew extensively, whereas the growth of most grains was inhibited, which is the characteristic of AGG. In Fig. 7(f), where ϵ is expected to be quite high, more pronounced AGG occurred with the growth of most matrix grains being inhibited. It should be noted that the matrix grains shown in Fig. 7(f) are much smaller than those shown in Fig. 7(e). Considering the matrix grains shown in Fig. 7(d)-(f), their size decreases with increasing Ti concentration, implying that the increase of ϵ inhibits grain growth. Besides, figures 7(d)-(f) show that the degree of AGG increases with increasing ϵ.

A similar effect of ϵ on the degree of AGG can also be found in the coarsening behavior of WC grains in the Co-rich liquid matrix. The triangular-prism shaped WC grains with truncated corners were observed to exhibit AGG in the WC-Co alloy, as shown in Fig. 8(a). When VC is added, however, the WC crystal shape changes into a triangular prism without corner truncation, and the overall grain growth rate was significantly reduced.[118] The shape change from a triangular prism with truncated corners to that without truncated corners indicates an increase in ϵ, as was discussed earlier. Although the overall growth rate is significantly reduced by the addition of 1 wt% VC, the size ratio of abnormally-growing large grains to small matrix grains increases markedly. This means that the role of VC is to increase ϵ, which retards the overall growth kinetics and increases the degree of AGG.

On the other hand, the nucleation barrier decreases markedly when 2-D nucleation takes place at the twin-plane reentrant edge (TPRE) instead of taking place on the defect-free terrace.[89,121–126] During the sintering of $BaTiO_3$, Schmelz *et al.*[125] observed that AGG is initiated by the twinning process. They monitored the growth of single- and double-twinned crystals, and demonstrated that only the latter could grow without limitation. Recent investigations on $BaTiO_3$[77,111] have shown that by sintering at 1350 °C, for instance, fine matrix grains usually less than $\sim 3\mu$m are replaced by abnormally grown coarse grains of $\sim 30\mu$m within a few minutes. Once fine matrix grains are completely replaced by coarse grains, further grain growth is retarded and a uniform grain size distribution is maintained. However, in the presence of a limited number of double-twinned grains, AGG was observed to take place again among those coarse grains.[111,127–130] This secondary AGG, which has been explained in terms of a growth advantage due to the TPRE,[128,129] was so marked

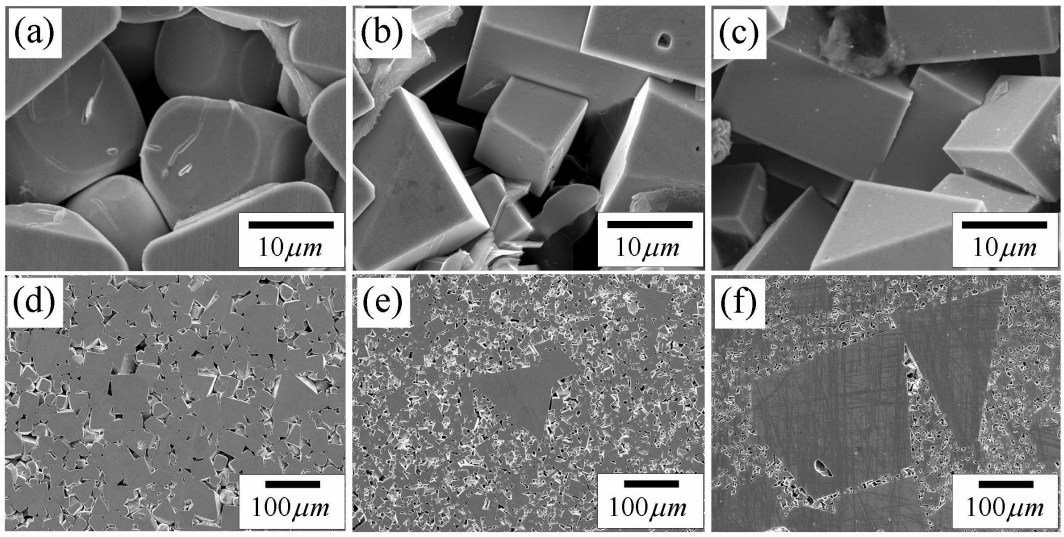

FIG. 7: SEM micrographs of $(Nb_{1-x}Ti_x)C$ grains and the microstructures of the $(Nb_{1-x}Ti_x)C$-Co specimens; (a) & (d) are when $x = 0$, (b) & (e) are when $x = 0.1$, and (c) & (f) are when $x = 0.25$.[114]

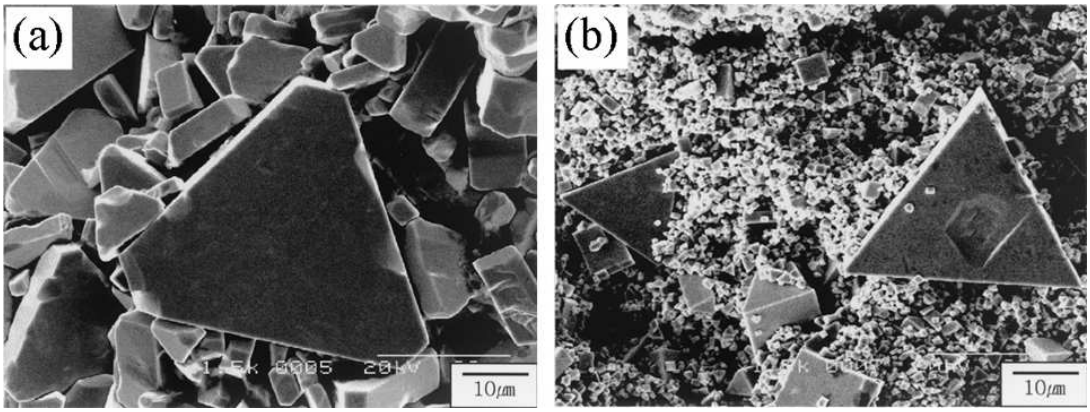

FIG. 8: SEM micrographs of WC grains after leaching out Co liquid phase from (a) WC-30Co and (b) WC-30Co-1VC (in wt%). Both specimens were sintered at 1500 °C for 72h under vacuum.[118]

that it has been used to fabricate $BaTiO_3$ single crystals larger than a few centimeters.[131] Furthermore, a very coarse grained microstructure could be obtained even in a heavily-donor-doped $BaTiO_3$ specimen by using seed particles with a double twin.[132] Note otherwise that grain growth is significantly limited when a donor is added to $BaTiO_3$.[133,134]

In $BaTiO_3$, a grain with a single twin does not grow perpetually because the reentrant edges are closed during grain growth. In the case of $Pb(Mg_{1/3}Nb_{2/3})O_3$-$PbTiO_3$ (PMN-PT) ceramics.[135–141], however, the grains even with a single twin grow preferentially and lead to AGG. Indeed, AGG occurring during the sintering of PMN-PT has been extensively studied to make a single crystal in a cost-effective way. For PMN-PT, it turned out that the twin characteristics are different *i.e.* a contact twin in $BaTiO_3$ and a penetration twin in PMN-PT. Since the reentrant edges due to the penetration twin are not closed, it can continue to provide a growth advantage via TPRE. Figure 9 shows a typical morphology of an abnormally grown twinned PMN-PT grain, and its detailed coarsening process has been treated elsewhere.[139]

During liquid-phase sintering, the formation of grain boundaries between grains in contact is usually observed because the dihedral angle is not always zero. As a consequence, grain boundary reentrant edges (GBREs) can be formed. Since the 2-D nucleation barrier at reentrant edges is lower, grain boundaries can also provide a preferential growth site like twins. It was proposed that the entrapment of small grains into an abnormal large grain observed in TaC[113] and in Al_2O_3[142] is a consequence of

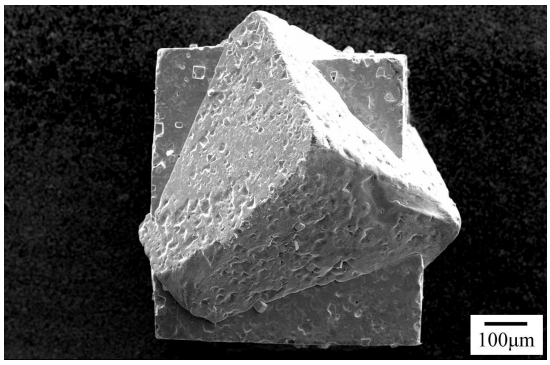

FIG. 9: Typical morphology of a twinned PMN-PT grain.[139]

GBRE enhanced coarsening processes. It was shown in $BaTiO_3$ system that a seed crystal without twins can also grow extensively up to as large as 5cm×5cm×1cm.[143] This exclusive growth of the seed grain without twins was attributed to the GBRE enhanced growth. It should be noted that the larger the grain size, the higher the probability of grain boundary formation with neighboring grains and the higher the growth rate by the GBRE mechanism.

On the other hand, abnormally-grown large grains in ceramic systems often have an elongated anisotropic shape,[73,78–83,93,144] which indicates that the growth rate of planes differs according to their crystallographic directions. For example, abnormally grown alumina grains typically show a hexagonal plate-like elongated shape,[82,83,93,145] which indicates that the growth rate of basal planes should be lower than that of non-basal planes. However, a liquid film is almost always present at the flat basal planes while the non-basal planes exhibit wetted as well as non-wetted boundaries.[146] Regarding the diffusion through liquid films, on the contrary, a fully-wetted basal plane is expected to grow faster than a partially-wetted non-basal plane. Therefore, it can be said that the growth rate of alumina planes is not a diffusion controlled process but an interface reaction controlled, *i.e.* 2-D nucleation. As long as the GBRE mechanism operates,[146,147] a liquid film coexisting with grain boundaries can migrate much faster than a liquid film without grain boundaries. The anisotropic shape of large alumina grains can be attributed to the enhanced nucleation process due to GBREs at non-basal planes.

B. Revisit to the Grain Growth Problems in Alumina

We can now reappraise one of the most famous research subjects in ceramic microstructure science *i.e.* the role of MgO during the sintering of Al_2O_3. Indeed, MgO-doped Al_2O_3[1] is not only a landmark in ceramic processing, but also a vehicle for the testing and development of the ceramic science. The MgO effect, particularly in relation to AGG, has been a long term research topic, which means that its role during the sintering of alumina is controversial.

Since the suppression of AGG during the sintering of Al_2O_3 ceramics by MgO addition is quite evident, its role has been mainly understood as a grain growth inhibitor and many studies have been devoted to understanding how the grain boundary migration is retarded. One of the most commonly accepted idea is the solute- or second-phase boundary pinning mechanism, as is well described in a review paper.[2] It was also proposed that the AGG of Al_2O_3 could be induced by an inhomogeneous densification behavior during sintering, caused by fluctuations in the green density.[148] In this respect, MgO can be regarded as a microstructure stabilizer or homogenizer that prevents inhomogeneous microstructural development.[149] When grain boundaries have anisotropic characteristics in terms of energy or mobility, local variation in densification or pore-boundary separation can occur, which could lead to AGG. Note that the addition of MgO has been found to narrow the distribution of the dihedral angles of the alumina surface, which indicates that the anisotropy of the surface and/or grain boundary energies is decreased by MgO.[150]

Inhomogeneous microstructural development can also be caused by impurities such as SiO_2, which is present ubiquitously during ceramic processing. Indeed, the presence of those liquid-forming impurities, even in extremely small amounts, was determined to be the cause of the AGG of alumina.[151,152] During sintering, impurities initially segregated at the grain boundaries are suggested to accumulate during grain growth. When the average grain size reaches a critical value, the impurity concentration exceeds the solubility limit and an intergranular liquid film emerges. AGG is supposed to be triggered by the appearance of a liquid. In this context, Gavrilov *et al.*[153] claimed that the important role of MgO in the sintering of alumina is a liquid-phase "scavenger". Handwerker *et al.*[154] also proposed that MgO enhances the solid solubility of liquid-forming impurities such as SiO_2.

An important fact which has not been considered in Al_2O_3 sintering is that almost all the commercial pure powders always have a small amount of impurities. Note also that the contamination during usual ceramic processing is difficult to avoid. A wide variety and diversity of experimental results obtained in Al_2O_3 sintering can be understood in terms of those uncontrolled impurities. In order to exclude the effect of those uncontrollable impurities and to make the alumina sintering as a single-phase process, Bae *et al.*[155] carried out experiments using ultra pure alumina powder (99.999%) and a sapphire crucible to prevent an impurity pick-up during sintering. It is interesting to note from their experiments that AGG, which is known to occur in "pure" alumina, was not detected even after the sintering at 1900 °C for 5h.

Since then, it has been confirmed many times that AGG does not occur even after the extensive sintering of a pure alumina specimen.[83,146,147,156–158] Figure 10 (a)

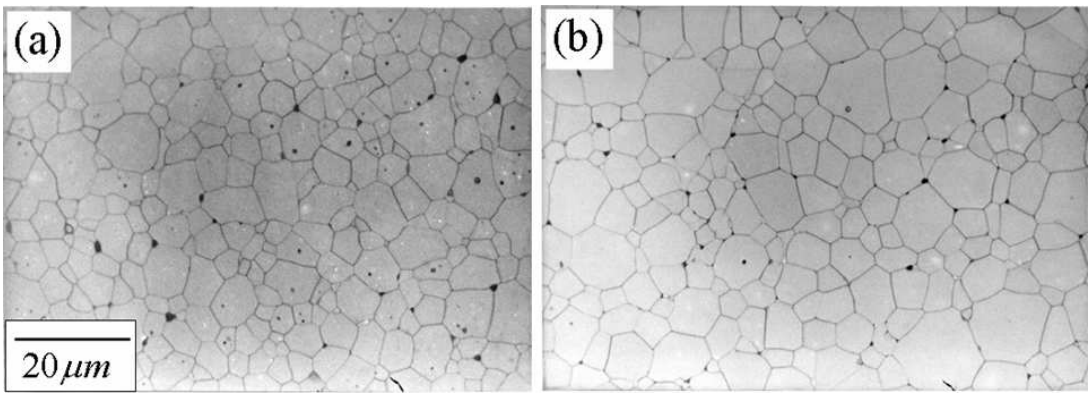

FIG. 10: Microstructures of (a) pure and (b) 500ppm-MgO-doped alumina specimens sintered at 1650 °C for 16h.

shows the microstructure of a pure alumina specimen obtained after sintering at 1650 °C for 16h, where no AGG occurs. Another important point to note is that the addition of MgO to pure alumina does not bring about a notable change in microstructure, as shown in Fig. 10 (b). Therefore, the AGG observed earlier in 'pure' alumina by Coble[1] is believed to be the result of the 'impure' initial powder used at that time.

Now the role of MgO, which prevents AGG during the sintering of alumina, may be attributed to the change in interface structure. Indeed, the vicinal (0001) surface of alumina was observed to show a hill-and-valley structure but it becomes atomically rough when heat-treated in an MgO atmosphere.[159] Besides, the flat solid-liquid interfaces in the alumina specimens prepared with an anorthite liquid ($CaAl_2Si_2O_8$) was also reported to be curved when the specimen was treated with MgO,[156,160,161] as shown in Figs. 11. These results strongly indicate that MgO lowers ϵ. With liquid-forming impurities such as SiO_2 and CaO, the interface structure of alumina is atomically smooth but is changed into atomically rough by MgO, and the grain growth behavior changes from an interface-reaction controlled to a diffusion controlled one.

The number of grains that can grow is expected to increase rapidly when the ϵ value of alumina crystals is lowered by MgO. Therefore, AGG with a bimodal grain size distribution may not appear. In this respect, MgO can be considered as a very effective grain growth promoter during the sintering of alumina. When its content is higher than 200 ppm, for instance, almost all the grains can grow and AGG is likely to be suppressed. Indeed, the effect of MgO is known to be noticeable during the sintering of alumina even when its concentration is not high enough to precipitate spinel. Greskovich *et al.*[162] showed that the solubility limit of MgO at 1880 °C in alumina is 175 ppm.

When the ϵ value of alumina crystals is lowered by MgO, it is further expected that, with an extremely small amount of MgO, AGG may appear rather significantly at an earlier stage of sintering. In that regard, Kim *et al.*[163] recently showed, with an alumina specimen prepared with 100 ppm SiO_2 and 100ppm CaO, that a significant AGG occurred in the 100-ppm-MgO added alumina specimen. However, a rather homogeneous and fine-grained microstructure was obtained in the 200-ppm-MgO added specimen. Dramatic differences in the microstructures of the specimen prepared with 0, 100 and 200 ppm MgO (Figs. 12(a)-(c)) can be noted. This indicates that the number of abnormally growing grains indeed increases quite rapidly with the increase in MgO concentration.

The well-known homogenizing effect of MgO[149] on the microstructural development of alumina can also be related to interface roughening by MgO. Note that roughening should result in a reduction or disappearance of the anisotropy in boundary energy and mobility. Furthermore, an increase in surface diffusivity by MgO addition[164,165] may also be the consequence of interface roughening. Ahn *et al.*[166] reported that the penetration kinetics of liquid (CaO + SiO_2) into the grain boundaries of alumina is significantly increased by MgO addition as a result of the roughened boundary structure. This means that during normal sintering, the liquid in the MgO-added specimen should distribute evenly at an early stage, resulting in a microstructure homogenization.

C. Grain Growth without Liquid Phase

Now let us consider the gain growth during solid state sintering, which is governed by the migration of grain boundaries. When we admit that grain boundaries have the same structural characteristics as other interfaces, it is not surprising that grain growth behavior is dependent on its atomic structure. Indeed, Cahn[54] has analyzed the thermodynamics of grain boundary and a possible phase transition. Rottman[167] also suggested that a grain-boundary roughening occurs with increasing temperature. Hsieh *et al.*[56] observed a roughening transition of grain boundaries of Al and Au by using hot stage electron microscopy during heating. Furthermore, curved boundaries were observed to transform again to sharply faceted

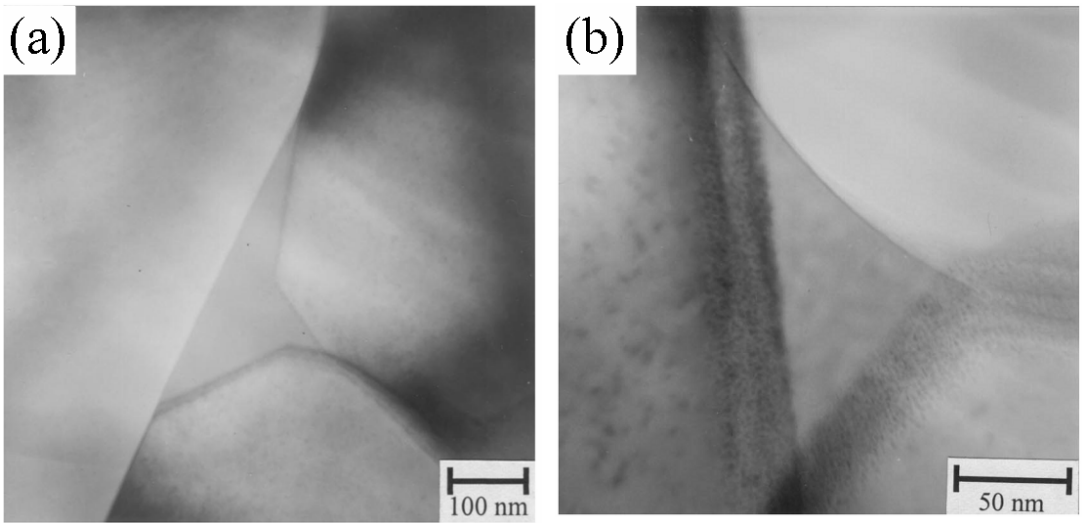

FIG. 11: TEM microstructures of a liquid pocket at a triple grain junction (a) with 1% anorthite and (b) with 1% anorthite and 2% MgO; sintered at 1620 °C for 10min.[158]

boundaries during cooling. An observation with high-resolution transmission electron microscopy (HRTEM) showed that a roughening transition of grain boundaries in a $SrTiO_3$ bicrystal occurs at about 1550 °C.[168] In addition, the grain-boundary structure of alumina was observed[169] to exhibit a reversible change from rough to smooth at temperatures below about 1100 °C. Ference *et al.*[55] showed that a reversible roughening transition of a Cu grain boundary occurs by the addition or removal of Bi impurity.

As already mentioned, grain boundaries in sintered ceramics are rather exception because the liquid-forming impurities almost always intervene during processing. However, sintering studies on Al_2O_3[156,158] and $BaTiO_3$[170–172] prepared carefully to minimize liquid phases showed a critical dependence of grain growth behavior on grain boundary structures. In analogy with the liquid-phase sintering, AGG was observed to occur only when the grain boundaries are faceted with an atomically smooth structure. It was reported that faceted grain-boundaries migrate by forming steps *i.e.* by 2-D nucleation-like process, and dislocations were determined to play a major role.[173,174] Recent HRTEM observation also confirmed that grain-boundary migration proceeds by a propagation of steps.[175]

In metallic systems, grain growth often occurs without liquid phase. In Fe-3%Si alloy, abnormally-growing grains, which are usually called "Goss", have a specific orientation of (110)[100] and make a strong texture. Hwang *et al.*[176,177] proposed that Goss grains grow by solid-state wetting along triple junctions of neighboring grains. A solid grain could wet or penetrate along grain boundaries or triple junctions if the anisotropy of grain boundary energy satisfies a wetting condition.

IV. DENSIFICATION DURING SINTERING

Alexander and Balluffi[178] clearly showed that grain boundaries act as a vacancy sink, and closed pores at the grain boundaries can be removed via grain boundary diffusion. When grain boundaries are rough, kink sites to which atoms can jump and attach are innumerable so that the energy barrier for the diffusion along grain boundaries becomes negligible. On the other hand, the diffusion along singular grain boundaries would be considerably sluggish, because the number of kinks is limited. It follows that the densification of systems with disordered grain boundaries is expected to be much easier than that of systems with ordered and singular grain boundaries. When the addition of a small amount of dopants leads to the changes in interface atomic structures, the densification during solid-state sintering will be enhanced or retarded.

One of the critical evidences demonstrating the role of the interface structure on densification can be found in tungsten. When the W powder compact is prepared with a very small amount of Ni, for instance, nearly full densification is achieved quite rapidly even at temperatures far below the liquid forming temperature. A similar phenomenon has also been reported in Mo, Ta and other refractory metals by the addition of Ni, Co or Fe. These are generally referred to as activated sintering.[180,181]

For the activated sintering of W by the addition of Ni, Hwang *et al.*[179] have demonstrated that the grains of pure W exhibit a polyhedral shape, *i.e.* atomically smooth surface, while those of Ni-doped show a spherical shape, *i.e.* atomically rough surface, as shown in Fig. 13. The grain boundaries were also observed to be faceted and defaceted in pure and Ni doped specimens, respectively. Based on the experimental results, they proposed

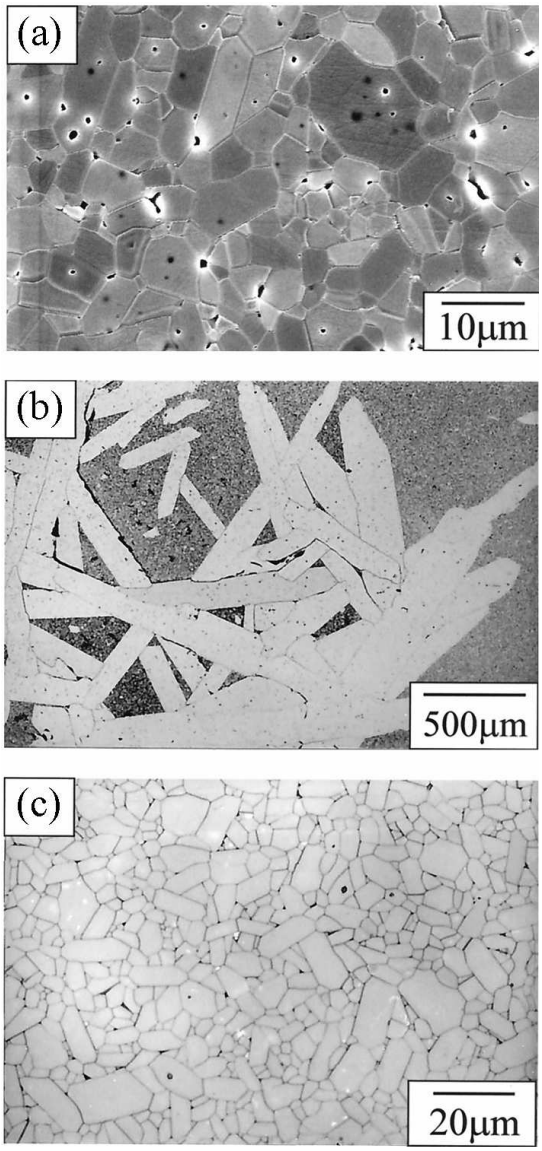

FIG. 12: Microstructures of the Al_2O_3 specimens containing 100ppm CaO and 100ppm SiO_2 sintered at 1650 °C for 8h: with (a) 0, (b) 100, and (c) 200ppm MgO.[163]

that the structural transition of the grain boundaries of W by Ni is the main cause of the rapid increase in the densification rate. Furthermore, Lee *et al.*[182] investigated the temperature dependence of the grain boundary diffusion in Ni-doped W, and found that the diffusivity increased abruptly at above ~ 1100 °C. These results were explained in relation to the grain boundary roughening transition.

It is believed that the correlation between the interface atomic structures and the densification process will be identical in metals and ceramics. Recently, Choi *et al.*[183] showed the dependence of densification behaviors on grain boundary structures in ceramic systems. From the fact that $BaTiO_3$ undergoes a grain boundary structural transition as a function of the oxygen partial pressure,[172] they monitored the difference in the microstructural evolution of $BaTiO_3$ ceramics as a function of the sintering atmosphere, and demonstrated that both the grain growth and the densification behavior depend critically on the interface atomic structure. These experimental evidences clearly suggest that the mass transport phenomena along grain boundaries are closely related to the structural characteristics of grain boundaries.

V. CONCLUDING REMARKS AND FUTURE DIRECTIONS

The grain growth and densification process during sintering were discussed in relation to the interface atomic structure. The abnormal grain growth of angular grains during liquid-phase sintering of ceramic materials was explained by considering that the grains having atomically smooth interfaces grow by 2-D nucleation mechanism. Based on the fact that the partially wetted surfaces can grow faster than the fully wetted surfaces in 2-D nucleation process, the development of the anisotropic abnormal grains was explained. It was proposed that the effect of additives, which retard or enhance the grain growth kinetics, can be approached by the step free energy concept. However, a detailed analysis on how the step free energy is affected by the additives is needed in future. On the other hand, it was shown that the grain boundary structure plays a critical role during solid state sintering because the pores are removed by the diffusion along the grain boundaries. This concept was applied to explain the enhancement in densification by the addition of a small amount of dopants.

Acknowledgments

The authors thank the reviewers for their helpful and constructive comments and are grateful for the financial support from the Ministry of Science and Technology of the Korean Government through the Creative Research Initiatives.

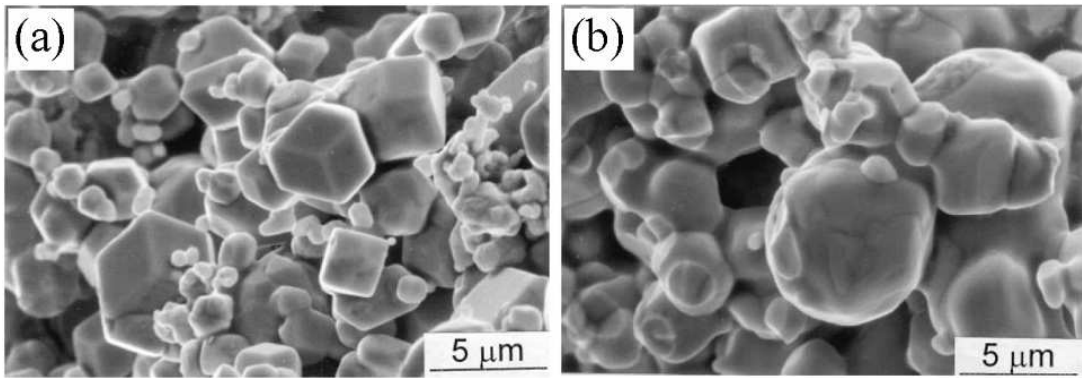

FIG. 13: SEM micrographs of the fractured surface of (a) pure W and (b) 0.4 wt% Ni doped W compacts after sintering at 1200 °C for 20 min in hydrogen.[179]

---

* corresponding author: dykim@snu.ac.kr

1. R. L. Coble, Transparent Alumina and Method of Preparation, U. S. Pat., No. 3 026 210, March 20, 1962 .
2. S. J. Bennison and M. P. Harmer, "A History of the Role of MgO in the Sintering of α-Al_2O_3"; pp. 13–49 in Ceramic Transactions, Vol. 7, *Sintering of Advanced Ceramics.* Edited by C. A. Handwerker, J. E. Blendell, and W. A. Kaysser. Am. Ceram. Soc., Westerville, 1990.
3. W. D. Kingery, H. K. Bowen, and D. R. Uhlmann, "Chapter 10. Grain Growth, Sintering and Vitrification"; pp. 448–513 in *Introduction to Ceramics,* John Wiley & Sons, Inc., New York, 1976.
4. R. M. German, *Sintering Theory and Practice,* John Wiley & Sons, Inc., New York, 1996 .
5. S.-J. L. Kang, *Sintering: Densification, Grain Growth & Microstructure,* Elsevier, Oxford, 2005 .
6. G. S. Rohrer, "Influence of Interface Anisotropy on Grain Growth and Coarsening," *Annu. Rev. Mater. Res.*, **35** 99–126 (2005).
7. C. Herring, "Effect of Change of Scale on Sintering Phenomena," *J. Appl. Phys.*, **21** 301–03 (1950).
8. C. Herring, "The Use of Classical Macroscopic Concepts in Surface-Energy Problems"; pp. 5–72 in *Structure and Properties of Solid Surfaces.* Edited by R. Gomer and C. S. Smith. University of Chicago Press, Chicago, 1953.
9. W. K. Burton, N. Cabrera, and F. C. Frank, "The Growth of Crystals and the Equilibrium Structure of Their Surfaces," *Phil. Trans. R. Soc.*, **243A** 299–358 (1951).
10. K. A. Jackson, "Nature of Solid-Liquid Interfaces"; pp. 319–24 in Proceedings of an International Conference on Crystal Growth, *Growth and Perfection of Crystals.* Edited by R. H. Doremus, B. W. Roberts, and D. A. Turnbull. John Wiley & Sons, Inc., New York, 1958.
11. D. P. Woodruff, *The Solid-Liquid Interface,* Cambridge University Press, London, 1973.
12. J. M. Howe, *Interfaces in Materials,* John Wiley & Sons, Inc., New York, 1997.
13. J. P. Hirth and G. M. Pound, "Growth and Evaporation of Dislocation-Free Crystals"; pp. 86–102 in Progress in Materials Science, Vol. 11, *Condensation and Evaporation.* Edited by B. Chalmers. Pergamon Press, Oxford, 1963.
14. I. V. Markov, *Crystal Growth for Beginners,* World Scientific Publishing Co. Pte. Ltd., Singapore, 1995.
15. J. W. Gibbs, "Chapter III. On the Equilibrium of Heterogeneous Substances"; pp. 55-349 in The Scientific Papers of J. Williard Gibbs, Vol I, *Thermodynamics.* Longmans, Green & Company, London, 1906.
16. P. Curie, "Sur la Formation des Crystaux et les Constants de Capillarité de leur Different Phase," *Bull. Soc. Franc. Minéral*, **8** 145–150 (1885).
17. G. Wulff, "Zur Frage der Geschwindigkeit des Wachsthums und der Auflösung der Krystallflächen," *Z. Krist.*, **34** 449–530 (1901).
18. M. von Laue, "Der Wulffsche Satz für die Gleichgewichtsform von Kristallen," *Z. Krist.*, **105** 124–33 (1943).
19. C. Herring, "Some Theorems on the Free Energies of Crystal Surfaces," *Phys. Rev.*, **82** 87–93 (1951).
20. J. W. Cahn and J. E. Taylor, "A Contribution to the Theory of Surface Energy Minimizing Shapes," *Scripta Metall.*, **18** 1117–20 (1984).
21. D. W. Hoffman and J. W. Cahn, "A Vector Thermodynamics for Anisotropic Surfaces–I. Fundamentals and Application to Plane Surface Junctions," *Surf. Sci.*, **31** 368–88 (1972).
22. J. W. Cahn and D. W. Hoffman, "A Vector Thermodynamics for Anisotropic Surfaces–II. Curved and Faceted Surfaces," *Acta Metall.*, **22** 1205–14 (1974).
23. C. Rottman and M. Wortis, "Equilibrium Crystal Shapes for Lattice Models with Nearest-and Next-Nearest-Neighbor Interactions," *Phys. Rev. B*, **29** [1] 328–39 (1984).
24. J. W. Cahn and C. A. Handwerker, "Equilibrium Geometries of Anisotropic Surfaces and Interfaces," *Mater. Sci. Eng.*, **A162** 83–95 (1993).
25. H. van Beijeren and I. Nolden, "Chapter 7. The Roughening Transition"; pp. 538–837 in *Structure and Dynamics of Surfaces II.* Edited by W. Schommers and P. von Blanckenhagen. Springer-Verlag, Berlin, 1987.
26. E. H. Conrad, "Surface Roughening, Melting and

Faceting," *Prog. Surf. Sci.*, **39** 65–116 (1992).
27. J. Lapujoulade, "The Roughening of Metal Surfaces," *Surf. Sci. Rep.*, **20** 191–249 (1994).
28. J. D. Weeks, "The Roughening Transition"; pp. 293–317 in *Ordering in Strongly Fluctuating Condensed matter Systems.* Edited by T. Riste. Plenum, New York, 1980.
29. H.-C. Jeong and E. D. Williams, "Steps on Surfaces: Experiment and Theory," *Surf. Sci. Rep.*, **34** 171–294 (1999).
30. R. J. Hamers, U. K. Köhler, and J. E. Demuth, "Epitaxial Growth of Silicon on Si(001) by Scanning Tunneling Microscopy," *J. Vac. Sci. Tech. A*, **8** [1] 195–200 (1990).
31. J. Wollschläger, E. Z. Luo, and M. Henzler, "Thermal Roughness of the Homogeneous and Inhomogeneous Cu(311) Surface Studied by High-Resolution Low-Energy Electron Diffraction," *Phys. Rev. B*, **44** [23] 13031–41 (1991).
32. S. Balibar, C. Guthmann, and E. Rolley, "From Vicinal to Rough Crystal Surfaces," *J. Phys. I (France)*, **3** [6] 1475–91 (1993).
33. H.-J. Ernst, R. Folkerts, and L. Schwenger, "Thermal Roughening of Cu(115): An Energy-Resolved Helium-Atom-Beam Scattering Study," *Phys. Rev. B*, **52** [11] 8461–70 (1995).
34. M. S. Hoogeman, D. C. Schlößer, J. B. Sanders, L. Kuipers, and J. W. M. Frenken, "Surface Energetics and Thermal Roughening of Ag(115) Studied with STM Movies," *Phys. Rev. B*, **53** [20] R13299–302 (1996).
35. S. T. Chui and J. D. Weeks, "Phase Transition in the Two-dimensional Coulomb Gas, and the Interfacial Roughening Transition," *Phys. Rev. B*, **14** [11] 4978–82 (1976).
36. A. Pimpinelli and J. Villain, *Physics of Crystal Growth,* Cambridge University Press, Cambridge, 1998.
37. E. E. Gruber and W. W. Mullins, "On the Theory of Anisotropy of Crystalline Surface Tension," *J. Phys. Chem. Solids*, **28** 875–87 (1967).
38. F. Gallet, S. Balibar, and E. Rolley, "The Roughening Transition of Crystal Surfaces. II. Experiments on Static and Dynamic Properties Near the First Roughening Transition of HCP ^{4}He," *J. Physique.*, **48** [11] 369–77 (1987).
39. W. Jo, "Chapter 4.3. On the Roughening Transition"; pp. 131–46 in Ph.D. Thesis, *Theoretical Analysis on the Equilibrium Shape of Crystals and Application to the Sintering Process.* Seoul National University, Seoul, 2005.
40. S. Surnev, K. Arenhold, P. Coenen, B. Voighlander, and H. P. Bonsel, "Scanning Tunneling Microscopy of Equilibrium Crystal Shapes," *J. Vac. Sci. Tech.*, **16** [3] 1059–65 (1998).
41. E. D. Williams and N. C. Bartelt, "Surface Faceting and the Equilibrium Crystal Shape," *Ultramicroscopy*, **31** 36–48 (1989).
42. E. D. Williams and N. C. Bartelt, "Thermodynamics of Surface Morphology," *Science*, **251** [4992] 393–400 (1991).
43. J. Prade, U. Schröder, W. Kress, F. W. de Wette, and A. D. Kulkarni, "Surface Relaxation, Surface Reconstruction and Surface Dynamics Close to the Antiferrodistortive Phase Transition of $SrTiO_3$(001) Slabs with Free SrO and TiO_2 Surfaces," *J. Phys.: Condens. Matter*, **5** 1–12 (1993).
44. H.-C. Jeong and J. D. Weeks, "The Dynamics of Steps on Vicinal Surfaces during Reconstruction-Driven Faceting," *Scan. Microsc.*, **12** [1] 17–29 (1998).
45. Ž. Crljen, P. Lazić, D. Šokčević, and R. Brako, "Relaxation and Reconstruction on (111) Surfaces of Au, Pt, and Cu," *Phys. Rev. B*, **68** [19] 195411 1–8 (2003).
46. D. Wolf, "Chapter 1. Materials Interfaes Atomic-Level Structure and Properties"; pp. 1–57 in *Materials Interfaces Atomic-Level Structure and Properties.* Edited by D. Wolf and S. Yip. Chapman & Hall, London, 1992.
47. L. E. Murr, *Interfacial Phenomena in Metals and Alloys,* Addison-Wesley, Massachusetts, 1975 .
48. W. T. Read and W. Shockley, "Dislocation Models of Crystal Grain Boundaries," *Phys. Rev.*, **78** [3] 275–89 (1950).
49. G. C. Hassen and C. Goux, "Interfacial Energies of Tilt Boundaries in Aluminum. Experimental and Theoretical Determination," *Scripta Metall.*, **5** [10] 889–94 (1971).
50. G. Hasson, J.-Y. Boos, I. Herbeuval, M. Biscondi, and G. Goux, "Theoretical and Experimental Determinations of Grain Boundary Structures and Energies: Correlation with Various Experimental Results," *Surf. Sci.*, **31** 115–37 (1972).
51. R. W. Balluffi, "Grain Boundary Diffusion Mechanisms in Metals," *Metall. Trans. A*, **13A** 2069–95 (1982).
52. D. Wolf, "Correlation between Structure, Energy, and Ideal Cleavage Fracture for Symmetrical Grain Boundaries in FCC Metals," *J. Mater. Res.*, **5** [8] 1708–30 (1990).
53. D. Wolf, "Structure and Energy of General Grain Boundaries in BCC Metals," *J. Appl. Phys.*, **69** [1] 185–96 (1991).
54. J. W. Cahn, "Transitions and Phase Equilibria Among Grain Boundary Structures," *J. Physique*, **43** [12] C6–199–213 (1982).
55. T. G. Ference and R. W. Balluffi, "Observation of a Reversible Grain Boundary Faceting Transition Induced by Changes of Composition," *Scripta Metall.*, **22** [12] 1929–34 (1988).
56. T. E. Hsieh and R. W. Balluffi, "Observation of Roughening/De-faceting Phase Transitions in Grain Boundaries," *Acta Metall.*, **37** [8] 2133–39 (1989).
57. A. P. Sutton and R. W. Balluffi, *Interfaces in Crystalline Solids,* Oxford University Press, Oxford, 1997.
58. J. H. Han, Y.-K. Chung, D.-Y. Kim, S.-H. Cho, and D. N. Yoon, "Temperature Dependence of the Shape of ZnO Grains in a Liquid Matrix," *Acta Metall.*, **37** [10] 2705–08 (1989).
59. S.-Y. Park, K. Choi, S.-J. L. Kang, and D. N. Yoon, "Shape of $MgAl_2O_4$ Grains in a CaMgSiAlO Glass Matrix," *J. Am. Ceram. Soc.*, **75** [1] 216–19 (1992).
60. R. M. German, *Liquid-Phase Sintering,* Plenum Press, New York, 1985.
61. D.-Y. Kim, S. M. Wiederhorn, B. J. Hockey, C. A. Handwerker, and J. E. Blendell, "Stability of Surface Energies of Wetted Grain Boundaries in Aluminum Oxide," *J. Am. Ceram. Soc.*, **77** [2] 444–53 (1994).
62. D. R. Clarke, "On the Equilibrium Thickness of Intergranular Glass Phases in Ceramic Materials," *J. Am. Ceram. Soc.*, **70** [7] 15–22 (1987).
63. I. M. Lifshitz and V. V. Slyozov, "The Kinetics of Precipitation from Supersaturated Solid Solutions," *J. Phys. Chem. Solids*, **19** 35–50 (1961).
64. C. Wagner, "Theory of Precipitate Change by Redissolution," *Z. Electrochem.*, **65** 581–91 (1961).

65. T.-K. Kang and D. N. Yoon, "Coarsening of Tungsten Grains in Liquid Nickel-Tungsten Matrix," *Metall. Trans. A*, **9** [3] 433–38 (1978).
66. G. C. Nicholson, "Grain Growth in MgO Containing a Liquid Phase," *J. Am. Ceram. Soc.*, **48** 525–28 (1965).
67. R. Warren, "Microstructural Development During the Liquid-Phase Sinteing of VC-Co Alloys," *J. Mater. Sci.*, **7** [12] 1434–42 (1972).
68. S. S. Kim and D. N. Yoon, "Coarsening Behavior of Mo Grains Dispersed in Liquid Matrix," *Acta Metall.*, **31** [8] 1151–57 (1983).
69. A. J. Ardell, "The Effect of Volume Fraction on Particle Coarsening: Theoretical Considerations," *Acta Metall.*, **20** [1] 61–71 (1972).
70. D.-Y. Kim and A. Accary, "Mechanisms of Grain Growth Inhibition During Sintering of WC-Co Based Hard-Metals," *Mater. Sci. Res.*, **13** 235–44 (1979).
71. J. Yang, D.-Y. Kim, and K.-Y. Eun, "Formation of Anomalous Large Grains in WC-Co Alloy Observed by Co Infiltration," *Powder Metall. Inter.*, **18** [2] 62–64 (1986).
72. A. Jaroenworaluck, T. Yamamoto, Y. Ikuhara, and T. Sakuma, "Segregation of vanadium at the WC/Co Interface in VC-doped WC-Co," *J. Mater. Res.*, **13** [9] 2450–52 (1998).
73. I.-K. Jeong, D.-Y. Kim, K. Z.-G, and S.-J. Kwon, "Exaggerated Grain Growth During the Sintering of Y-Ba-Cu-O Superconducting Ceramics," *Mater. Lett.*, **8** [3,4] 91–94 (1989).
74. H.-H. Yoon and D.-Y. Kim, "Effect of Heating Rate on the Exaggerated Grain Growth During the Sintering of Sr-Hexaferrite," *Mater. Lett.*, **20** [3,4] 293–97 (1994).
75. G. R. Chol, "Influence of Milled Powder Particle Size Distribution on the Microstructure and Electrical Properties of Sintered Mn-Zn Ferrites," *J. Am. Ceram. Soc.*, **54** [1] 34–39 (1971).
76. D. F. K. Henning, R. Janssen, and P. J. L. Reynen, "Control of Liquid-Phase Enhanced Discontinuous Grain Growth in Barium Titanate," *J. Am. Ceram. Soc.*, **70** [1] 23–27 (1987).
77. Y. S. Yoo, H. Kim, and D.-Y. Kim, "Effect of SiO_2 and TiO_2 Addition on the Exaggerated Grain Growth of $BaTiO_3$," *J. Eur. Ceram. Soc.*, **17** [7] 905–11 (1997).
78. S. J. L. Kang and S. M. Han, "Grain Growth in Si_3N_4 Based Materials," *MRS Bull.*, **20** 33–37 (1995).
79. S.-H. Rhee, J. D. Lee, and D.-Y. Kim, "Effect of β-Seed Addition on the Microstructural Evolution of Silicon Nitride Ceramics," *J. Am. Ceram. Soc.*, **84** [12] 3040–42 (2001).
80. A. H. Heuer, G. A. Fryburg, L. U. Ogbuji, T. E. Mitchell, and S. Shinozaki, "β-α Transformation in Polycrystalline SiC: I. Microstructural Aspects," *J. Am. Ceram. Soc.*, **61** [9] 406–12 (1978).
81. Y. W. Kim, J.-Y. Kim, S.-H. Rhee, and D.-Y. Kim, "Effects of Initial Particle Size on Microstructure of Liquid-Phase Sintered Silicon Carbide," *J. Eur. Ceram. Soc.*, **20** [7] 945–49 (2000).
82. H. Song and R. L. Coble, "The Origin of Growth Kinetics of Platelike Abnomal Grains in Liquid-Phase-Sintered Alumina," *J. Am. Ceram. Soc.*, **73** [7] 2077–85 (1990).
83. S.-H. Hong and D.-Y. Kim, "Effect of Liquid Content on the Abnormal Grain Growth of Alumina," *J. Am. Ceram. Soc.*, **84** [7] 1597–600 (2001).
84. S. Prochazka, S. L. Dole, and C. I. Hejna, "Abnormal grain Growth and Microcracking in Boron Carbide," *J. Am. Ceram. Soc.*, **68** [9] C235–36 (1985).
85. S. H. Hong and G. L. Messing, "Anisotropic Grain Growth in Diphasic-Gel Derived Titania-Doped Mullite," *J. Am. Ceram. Soc.*, **81** [5] 1269–77 (1998).
86. K.-S. Oh, J.-Y. Jun, D.-Y. Kim, and N. M. Hwang, "Shape Dependence of the Coarsening Behavior of NbC Grains Dispersed in a Liquid Iron Matrix," *J. Am. Ceram. Soc.*, **83** [12] 3177–220 (2000).
87. G. J. Shiflett, H. I. Aaronson, and T. H. Courtney, "Kinetics of Coarsening by the Ledge Mechanism," *Acta Metall.*, **27** [3] 377–85 (1979).
88. S. D. Peteves and R. Abbaschian, "Growth Kinetics of Solid-Liquid Ga Interfaces: Part II. Theoretical," *Metall. Trans. A*, **22A** 1271–86 (1991).
89. W. A. Tiller, "Chapter 2.2.2. Layer Source-Limited Kinetics"; pp. 80–84 in *The Science of Crystallization: Microscopic interfacial Phenomena.* Cambridge University Press, New York, 1991.
90. P. Wynblatt and N. A. Gjostein, "Particle Growth in Model Supported Metal Catalysts-I. Theory," *Acta Metall.*, **24** [12] 1165–74 (1976).
91. A. Searcy, "Driving Force for Sintering of Particles with Anisotropic Surface Energies," *J. Am. Ceram. Soc.*, **68** [10] C–267–C–268 (1985).
92. Y. J. Park, N. M. Hwang, and D. Y. Yoon, "Abnormal Growth of Faceted (WC) Grains in a (Co) Liquid Matrix," *Metall. Trans. A*, **27A** [9] 2809–19 (1996).
93. J. Rödel and A. M. Glaeser, "Anisotropy of Grain Growth in Alumina," *J. Am. Ceram. Soc.*, **73** [11] 3292–301 (1990).
94. M. M. Seabaugh, I. H. Kerscht, and G. L. Messing, "Texture Development by Templated Grain Growth in Liquid-Phase Sintered α Alumina," *J. Am. Ceram. Soc.*, **80** [5] 11–81–88 (1997).
95. J. Rankin and B. W. Sheldon, "Surface Roughening and Unstable Neck Formation in Faceted Particles: I. Experimental Results and Mechanisms," *J. Am. Ceram. Soc.*, **82** [7] 1868–72 (1999).
96. B. W. Sheldon and J. Rankin, "Surface Roughening and Unstable Neck Formation in Faceted Particles: II. Mathematical Modeling," *J. Am. Ceram. Soc.*, **82** [7] 1873–81 (1999).
97. A. D. Rutenberg and B. P. Vollmayr-Lee, "Anisotropic Coarsening: Grain Shapes and Nonuniversal Persistence," *Phys. Rev. Lett.*, **83** [19] 3772–75 (1999).
98. M. Kitayama, T. Narushima, and A. M. Glaeser, "The Wulff Shape of Alumina: II. Experimental measurements of Pore Shape Evolution Rates," *J. Am. Ceram. Soc.*, **83** [10] 2572–83 (2000).
99. W. W. Mullins and G. S. Rohrer, "Nucleation Barrier for Volume-Conserving Shape Changes of Faceted Crystals," *J. Am. Ceram. Soc.*, **83** [1] 214–16 (2000).
100. P. W. Rehrig, G. L. Messing, and S. Trolier-McKinistry, "Templated Growth of Barium Titanate Single Crystals," *J. Am. Ceram. Soc.*, **83** [11] 2654–60 (2000).
101. E. Brosh and R. Z. Shneck, "Anisotropic Coarsening: the Effect of Interfacial Properties on the Shape of the Grains," *Modelling Simul. Mater. Sci. Eng.*, **8** 815–23 (2000).
102. T. Kuroda, T. Irisawa, and A. Ookawa, "Growth of a Polyhedral Crystal from Solution and its Morphological Stability," *J. Cryst. Growth*, **42** 41–46 (1977).
103. P. Bennema and J. P. van der Earden, "Crystal Growth

from Solution: Development in Computer Simulation," *J. Cryst. Growth*, **42** 201–13 (1977).
104. I. Sunagawa, "Chapter 7. Morphology of Minerals"; pp. 509–87 in *Morphology of Crystals, Part B.* Edited by I. Sunagawa. Terra Sci. Pub., Tokyo, 1987.
105. I. Sunagawa, "The Distinction of Natural from Synthetic Diamonds," *J. Gemm.*, **24** [7] 485–99 (1995).
106. J. W. Cahn, W. B. Hillig, and G. W. Sears, "The Molecular Mechanism of Solidification," *Acta Metall.*, **12** [12] 1421–39 (1964).
107. S. D. Peteves and R. Abbaschian, "Growth Kinetics of Solid-Liquid Ga Interfaces: Part I. Experilmental," *Metall. Trans. A*, **22A** 1259–70 (1991).
108. M.-K. Kang, D.-Y. Kim, and N. M. Hwang, "Ostwald Ripening Kinetics of Angular Grains Dispersed in a Liquid Phase by 2-Dimensional Nucleation and Abnormal Grain Growth," *J. Eur. Ceram. Soc.*, **22** [5] 603–12 (2002).
109. B. W. Sheldon and J. Rankin, "Step-Energy Barriers and Particle Shape Changes during Coarsening," *J. Am. Ceram. Soc.*, **85** [3] 683–90 (2002).
110. G. S. Rohrer, C. L. Rohrer, and W. W. Mullins, "Coarsening of Faceted Crystals," *J. Am. Ceram. Soc.*, **85** [3] 675–82 (2002).
111. M.-K. Kang, Y.-S. Yoo, D.-Y. Kim, and N.-M. Hwang, "Growth of $BaTiO_3$ Seed Grains by the Twin Plane Reentrant Edge Mechanism," *J. Am. Ceram. Soc.*, **83** [2] 385–90 (2000).
112. S.-G. Kwon, S.-H. Hong, N.-M. Hwang, and D.-Y. Kim, "Coarsening Behavior of Growth of C_3S and C_2S Grains Dispersed in a Clinker Melt," *J. Am. Ceram. Soc.*, **83** [5] 1247–52 (2000).
113. K. Choi, J.-W. Choi, D.-Y. Kim, and N.-M. Hwang, "Effect of Coalescence on the Grain Coarsening during Liquid-Phase Sintering of TaC-TiC-Ni Cermets," *Acta Mater.*, **48** [12] 3125–29 (2000).
114. K. Choi, N.-M. Hwang, and D.-Y. Kim, "Effect of Grain Shape on Abnormal Grain Growth in Liquid-Phase-Sintered (Nb,Ti)C-Co Alloys," *J. Am. Ceram. Soc.*, **85** [9] 2313–18 (2002).
115. W. Jo, U.-J. Chung, N. M. Hwang, and D.-Y. Kim, "Temperature Dependence of the Coarsening Behavior of (Ba, Sr)TiO_3 Grains Dispersed in a SiO_2-Rich Liquid Matrix," *J. Eur. Ceram. Soc.*, **23** [10] 1565–69 (2003).
116. S.-Y. Chung, D. Y. Yoon, and S.-J. L. Kang, "Effect of Donor Concentration and Oxygen Partial Pressure on Interface Morphology and Grain Growth Behavior in $SrTiO_3$," *Acta Mater.*, **50** [13] 3361–71 (2002).
117. P. Wynblatt, "Particle Growth in Model Supported Metal Catalysts-II. Comparison of Experiment with Theory," *Acta Metall.*, **24** [12] 1175– 81 (1976).
118. H. R. Lee, D. J. Kim, N. M. Hwang, and D.-Y. Kim, "Role of VC Additive during Sintering of WC-Co: Mechanism of Grain Growth Inhibition," *J. Am. Ceram. Soc.*, **86** [1] 152–54 (2003).
119. S. Y. Chung and S. J. L. Kang, "Effect of Dislocations on Grain Growth in Strontium Titanate," *J. Am. Ceram. Soc*, **83** [11] 2828–32 (2000).
120. S. Y. Chung and S. J. L. Kang, "Intergranular Amorphous FIlms and Dislocations-Promoted Grain Growth in $SrTiO_3$," *Acta Mater*, **51** [8] 2345–54 (2003).
121. R. S. Wagner, "On the Growth of Germanium Dendrites," *Acta Metall.*, **8** [1] 57–60 (1960).
122. D. R. Hamilton and R. G. Seidensticker, "Propagation Mechanism of Germanium Dendrites," *J. Appl. Phys.*, **31** [7] 1165–68 (1960).
123. J. F. Hamilton and L. E. Brady, "Twinning and Growth of Silver Bromide Microcrystals," *J. Appl. Phys.*, **35** [2] 414–21 (1964).
124. D. Elwell and H. J. Scheel, *Crystal Growth from High-Temperature Solutions,* Academic Press, London, 1975.
125. H. Schmelz and A. Meyer, "The Evidence for Anomalous Grain Growth Below the Eutectic Temperature in $BaTiO_3$ Ceramics," *Ceram. Forum Int. Ber. Dtsch. Keram. Ges*, **59** [8/9] 436–40 (1982).
126. N.-B. Ming and I. Sunagawa, "Twin Lamellae as Possible Self-Perpetuating Step Sources," *J. Cryst. Growth*, **87** [1] 13–17 (1988).
127. M.-G. Kang, D.-Y. Kim, H.-Y. Lee, and N. M. Hwang, "Temperature Dependence of the Coarsening Behavior of Barium Titanate Grains," *J. Am. Ceram. Soc*, **83** [12] 3202–04 (2000).
128. H. Y. Lee, J. S. Kim, N. M. Hwang, and D. Y. Kim, "Effect of Sintering Temperature on the Secondary Abnormal Grain Growth of $BaTiO_3$," *J. Eur. Ceram. Soc*, **20** [6] 731–37 (2000).
129. H. Y. Lee, J. S. Kim, and D. Y. Kim, "Effect of Twin-Plane Renetrant Edge on the Coarsening Behavior of Barium Titanate Grains," *J. Am. Ceram. Soc*, **85** [4] 977–80 (2002).
130. H.-R. Jin, W. Jo, N.-M. Hwang, and D.-Y. Kim, "Coarsening Advantage of Twinned $BaTiO_3$ Seed Particle," *J. Kor. Ceram. Soc.*, **42** [9] 599–601 (2005).
131. H. Y. Lee, J. S. Kim, and D. Y. Kim, "Fabrication of $BaTiO_3$ Single Crystals Using Secondary Abnormal Grain Growth," *J. Eur. Ceram. Soc*, **20** [10] 1595–97 (2000).
132. B. K. Park, J. H. Lee, D. Y. Kim, and N. M. Hwang, "Positive Temperature Coefficient of Resistance Effect in Heavily Nb-Doped Barium Titanate by the Growth of the Double-Twinned Seeds," *J. Am. Ceram. Soc*, **84** [44] 2707–09 (2001).
133. M. Drofenik, "Oxygen Partil Pressure and Grain Growth in Donor-Doped $BaTiO_3$," *J. Am. Ceram. Soc.*, **70** [5] 311–14 (1987).
134. H. M. Chan, M. P. Harmer, and D. M. Smyth, "Compensating Defects in Highly Donor-Doped $BaTiO_3$," *J. Am. Ceram. Soc.*, **69** [6] 507–10 (1986).
135. A. Khan, D. T. Carpenter, A. M. Scotch, H. M. Chan, and M. P. Harmer, "Electrom Back Scatter Diffraction Analysis of $Pb(Mg_{1/3}\ Nb_{2/3})O_3$-35mol% $PbTiO_3$ Single Crystals Grown by Seeded Polycrystal Conversion," *J. Mater. Res.*, **16** [3] 694–700 (2001).
136. U.-J. Chung, J.-K. Park, D.-Y. Kim, N. M. Hwang, and H.-Y. Lee, "Effect of Grain Coalescence on the Abnormal Grain Growth of PMN-35PT Ceramics," *J. Am. Ceram. Soc.*, **85** [4] 965–68 (2002).
137. J. S. Wallace, J.-M. Huh, J. E. Blendell, and C. A. Handwerker, "Grain Growth and Twin Formation in 0.74PMN-0.26PT," *J. Am. Ceram. Soc.*, **85** [6] 1581–84 (2002).
138. U.-J. Chung, J.-K. Park, N. M. Hwang, H.-Y. Lee, and D.-Y. Kim, "Abnormal Grain Growth of PMN-35PT Ceramics Induced by the Penetration Twin," *J. Am. Ceram. Soc.*, **85** [12] 3076–80 (2002).
139. U.-J. Chung, W. Jo, J.-H. Lee, N. M. Hwang, and D.-Y. Kim, "Coarsening Process of the Penetration Twinned $Pb(Mg_{1/3}\ Nb_{2/3})O_3$-35 mol%$PbTiO_3$ Grain," *J. Am.*

Ceram. Soc., **87** [1] 125–28 (2004).
140. W. Jo, U.-J. Chung, N. M. Hwang, and D.-Y. Kim, "Effect of SiO_2 and TiO_2 Addition on the Morphology of Abnormally Grown Large PMN-35mol/Grains," *J. Am. Ceram. Soc.*, **88** [7] 1992–94 (2005).
141. J. G. Fisher, M.-S. Kim, H.-Y. Lee, and S.-J. L. Kang, "Effect of Li_2O and PbO Additions on Abnormal Grain Growth in the $Pb(Mg_{1/3}Nb_{2/3})O_3$-35 mol% $PbTiO_3$ System," *J. Am. Ceram. Soc.*, **87** [5] 937–42 (2004).
142. S.-H. Lee, D.-Y. Kim, and N.-M. Hwang, "Effect of Anorthite Liquid on the Abnormal Grain Growth of Alumina," *J. Eur. Ceram. Soc.*, **22** [3] 317–21 (2002).
143. H.-Y. Lee, "Solid-State Single Crystal Growth (SSCG) Method: A Cost-Effective Way of Growing Piezoelectric Single Crystals"; pp. 160–77 in *Piezoelectric Single Crystals and Their Application.* Edited by S. Trolier-McKinstry, Y. Yamashita, and L. E. Cross. PSU, PA, 2004.
144. M. Kitayama, K. Hirao, M. Toriyama, and S. Kansaki, "Experimental Evidence for the Anisotropic Ostwald Ripening of β-Silicon Nitride," *J. Am. Ceram. Soc.*, **82** [10] 2931–33 (1999).
145. H. Song and R. L. Coble, "Morphology of Platelike Abnormal Grains in Liquid-Phase-Sintered Alumina," *J. Am. Ceram. Soc.*, **73** [7] 2086–90 (1990).
146. O.-S. Kwon, S.-H. Hong, J.-H. Lee, U.-J. Chung, D.-Y. Kim, and N.-M. Hwang, "Microstructural Evolution During Sintering of TiO_2/SiO_2-Doped Alumina: Mechanism of Anisotropic Abnormal Grain Growth," *Acta Mater.*, **50** [19] 4865–72 (2002).
147. Y.-M. Kim, S.-H. Hong, and D.-Y. Kim, "Anisotropic Abnormal Grain Growth in TiO_2/SiO_2-Doped Alumina," *J. Am. Ceram. Soc*, **83** [11] 2809–12 (2000).
148. R. E. Mistler and R. L. Coble, "Microstructural Variation Due to Fabrication," *J. Am. Ceram. Soc.*, **51** [4] 237–40 (1968).
149. N. J. Shaw and R. J. Brook, "Structure and Grain Coarsening During Sintering of Alumina," *J. Am. Ceram. Soc.*, **69** [2] 107–10 (1986).
150. C. A. Handwerker, J. M. Dynys, R. M. Cannon, and R. L. Coble, "Dihedral Angles in Magnesia and Alumina: Distributions from Surface Thermal Grooves," *J. Am. Ceram. Soc.*, **73** [5] 1371–77 (1990).
151. S. I. Bae and S. Baik, "Determination of Critical Concentrations of Silica and/or Calcia for Abnormal Grain Growth in Alumina," *J. Am. Ceram. Soc.*, **76** [4] 1065–67 (1993).
152. W. A. Kaysser, M. Sprissler, C. A. Handwerker, and J. E. Blendell, "Effect of a Liquid Phase on the Morphology of Grain Growth in Alumina," *J. Am. Ceram. Soc.*, **70** [5] 339–43 (1987).
153. K. L. Gavrilov, S. J. Bennison, K. R. Mikeska, J. M. Chabala, and R. L. Setti, "Silica and Magnesia Dopant Distributions in Alumina by High Resolution Scanning Secondary Ion Mass Spectrometry," *J. Am. Ceram. Soc.*, **82** [4] 1001–08 (1999).
154. C. A. Handwerker, P. A. Morris, and R. L. Coble, "Effect of Chemical Inhomogeneities on Grain Growth and Microstructure in Al_2O_3," *J. Am. Ceram. Soc.*, **72** [1] 130–36 (1996).
155. S. I. Bae and S. Baik, "Sintering and Grain Growth of Ultrapure Alumina," *J. Mater. Sci.*, **28** [15] 4197–204 (1993).
156. C. W. Park and D. Y. Yoon, "Effect of SiO_2, CaO, and MgO Additions on the Grain Growth of Alumina," *J. Am. Ceram. Soc.*, **83** [10] 2605–09 (2000).
157. T.-W. Sone, J.-H. Han, S.-H. Hong, and D.-Y. Kim, "Effect of Surface Impurities on the Microstructure Development during Sintering of Alumina," *J. Am. Ceram. Soc.*, **84** [6] 1386–88 (2001).
158. C. W. Park and D. Y. Yoon, "Abnormal Grain Growth in Alumina with Anorthite Liquid and the Effect of MgO Addition," *J. Am. Ceram. Soc.*, **85** [6] 1585–93 (2002).
159. C. W. Park and D. Y. Yoon, "Effect of MgO on Faceted Vicinal (0001) Surface of Aluminum Oxide," *J. Am. Ceram. Soc.*, **84** [2] 456–58 (2001).
160. M.-J. Kim and D. Y. Yoon, "Effect of MgO Addition on Surface Roughening of Alumina Grains in Anorthite Liquid," *J. Am. Ceram. Soc.*, **86** [4] 630–33 (2003).
161. C. W. Park, D. Y. Yoon, J. E. Blendell, and C. A. Handwerker, "Singular Grain Boundaries in Alumina and Their Roughening Transition," *J. Am. Ceram. Soc.*, **86** [4] 603–11 (2003).
162. C. Greskovich and J. A. Brewer, "Solubility of MgO in Polycrystalline Alumina at High Temperatures," *J. Am. Ceram. Soc.*, **84** [2] 420–25 (2001).
163. B.-K. Kim, S.-H. Hong, D.-Y. Kim, and N.-M. Hwang, "Alternative Explanation for the Role of MgO in the Sintering of Alumina Containing mall Amounts of a Liquid Phase," *J. Am. Ceram. Soc.*, **86** [4] 634–39 (2003).
164. K. A. Berry and M. P. Harmer, "Effect of MgO Solute on Microstructure Development in Al_2O_3," *J. Am. Ceram. Soc.*, **70** [9] 682–88 (1987).
165. J. Rödel and A. M. Glaeser, "Pore Drag and Pore-Boundary Separation in Alumina," *J. Am. Ceram. Soc.*, **73** [11] 3302–12 (1990).
166. J. H. Ahn, J.-H. Lee, S.-H. Hong, N.-M. Hwang, and D.-Y. Kim, "Effect of Liquid-Forming Additive Content on the Kinetics of Abnormal Grain Growth in Alumina," *J. Am. Ceram. Soc.*, **86** [8] 1421–23 (2003).
167. C. Rottman, "Roughening of Low-Angle Grain Boundaries," *Phys. Rev. Lett.*, **57** [6] 735–38 (1986).
168. S. B. Lee, W. Sigle, and M. Rhule, "Faceting of an Asymmetric $SrTiO_3$ 5[001] Tilt Grain Boundary Close to Its Defaceting Transition," *Acta Mater.*, **51** [15] 4583–88 (2003).
169. M.-J. Kim, Y. K. Cho, and D. Y. Yoon, "Facet and Defacet Transition of Grain Boundaries of Alumina," *J. Am. Ceram. Soc.*, **87** [3] 455–59 (2004).
170. S. B. Lee, S.-Y. Choi, S.-J. L. Kang, and D. Y. Yoon, "TEM Observations of Singular Grain Boundaries and Their Roughening Transition in TiO_2-Excess $BaTiO_3$," *Z. Metallkd.*, **94** [3] 193–99 (2003).
171. Y.-I. Jung, S.-Y. Choi, and S.-J. L. Kang, "Grain-Growth Behavior during Stepwise Sintering of Barium Titanate in Hydrogen Gas and Air," *J. Am. Ceram. Soc.*, **86** [12] 2228–30 (2003).
172. B.-K. Lee, S.-Y. Chung, and S.-J. L. Kang, "Grain Boundary Faceting and Abnormal Grain Growth in $BaTiO_3$," *Acta Mater.*, **48** [7] 1575–80 (2000).
173. H. Gleiter, "The Mechanism of Grain Boundary Migration," *Acta Metall.*, **17** [5] 565–73 (1969).
174. C. M. F. Rae and D. A. Smith, "On the Mechanisms of Grain Boundary Migration," *Phil. Mag.*, **41A** [4] 477–92 (1980).
175. K. L. Merkle and L. J. Thompson, "Atomic-scale Observation of Grain Boundary Motion," *Mater. Lett.*, **48** [3,4] 188–93 (2001).

176. N. M. Hwang, "Grain Growth Behavior in the System of Anisotropic Grain Boundary Mobility," *Scipta Mater.*, **37** [11] 1637 (1997).
177. H. Park, D. Y. Kim, and N. M. Hwang, "Microstructural Evidence of Abnormal Grain Growth by Solid-State Wetting in Fe-3%Si Steel," *J. Appl. Phys.*, **95** [10] 5515–21 (2004).
178. B. H. Alexander and R. W. Balluffi, "The Mechanism of Sintering of Copper," *Acta Metall.*, **5** [11] 666–77 (1957).
179. N. M. Hwang, Y. J. Park, D.-Y. Kim, and D. Y. Yoon, "Activated Sintering of Ni-Doped Tungsten: Approach by Grain Boundary Structural Transition," *Scripta Metall.*, **42** [5] 421–25 (2000).
180. I. J. Toth and N. A. Lockington, "The Kinetics of Metallic Activation Sintering of Tungsten," *J. Less Common Metals*, **12** [5] 353–65 (1967).
181. G. H. Gessinger and H. F. Fischmeister, "A model for Second-Stage Liquid-Phase Sintering with a Partially Wetting Liquid," *Acta Metall*, **21** [5] 715–24 (1973).
182. J. S. Lee, K. Klockgeter, and C. Herzig, "Grain Boundary Self and Impurity Diffusion in Tungsten in the Temperature Range of Activated Sintering," *J. Phys. Colloq*, **C1** [1] 569–74 (1990).
183. S.-Y. Choi and S.-J. L. Kang, "Sintering Kinetics by Structural Transition at Grain Boundaries in Barium Titanate," *Acta Mater.*, **52** [10] 2937–43 (2004).